AD-A112 338 MASSACHUSETTS INST OF TECH LEXINGTON LINCOLN LAB F/G 5/8
EXPOSING OBJECTS UNDER LIGHT CLOUD COVER BY ADAPTIVE HOMOMORPHI--ETC(U)
JAN 82 T PELI, T F QUATIERI F19628-80-C-0002
UNCLASSIFIED TR-587 ESD-TR-81-363 NL

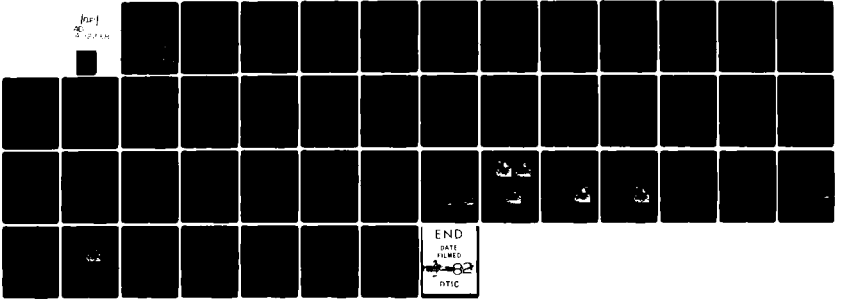

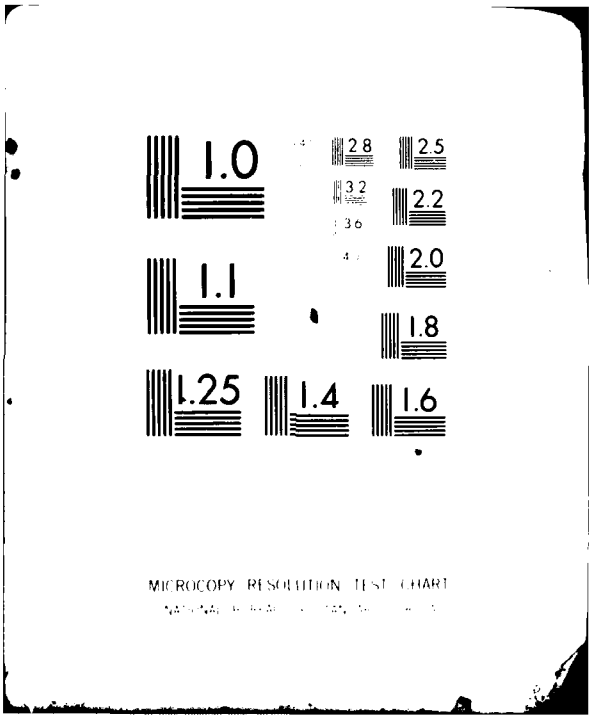
1.0
2.8
2.5
3.2
2.2
3.6
2.0
1.1
1.8
1.25
1.4
1.6
MICROCOPY RESOLUTION TEST CHART

ESD-TR-81-363

(12)

Technical Report

587

T. Peli
T.F. Quatieri

Exposing Objects Under Light Cloud Cover by Adaptive Homomorphic Filtering

6 January 1982

Prepared for the Department of the Air Force
under Electronic Systems Division Contract F19628-80-C-0002 by

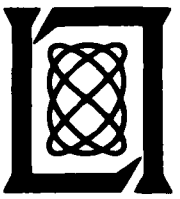

Lincoln Laboratory

MASSACHUSETTS INSTITUTE OF TECHNOLOGY

Lexington, Massachusetts

The work reported in this document was performed at Lincoln Laboratory, a center for research operated by Massachusetts Institute of Technology, with the support of the Department of the Air Force under Contract F19628-80-C-0002. A part of this support was provided by the Rome Air Development Center.

The Public Affairs Office has reviewed this report, and it is releasable to the National Technical Information Service, where it will be available to the general public, including foreign nationals.

This technical report has been reviewed and is approved for publication.

FOR THE COMMANDER

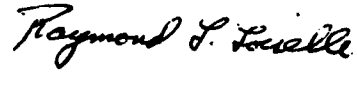

Raymond L. Loiselle, Lt.Col., USAF
Chief, ESD Lincoln Laboratory Project Office

Non-Lincoln Recipients

PLEASE DO NOT RETURN

Permission is given to destroy this document when it is no longer needed.

MASSACHUSETTS INSTITUTE OF TECHNOLOGY
LINCOLN LABORATORY

EXPOSING OBJECTS UNDER LIGHT CLOUD COVER BY ADAPTIVE HOMOMORPHIC FILTERING

T. PELI
T.F. QUATIERI
Group 27

TECHNICAL REPORT 587

6 JANUARY 1982

LEXINGTON MASSACHUSETTS

i/ii

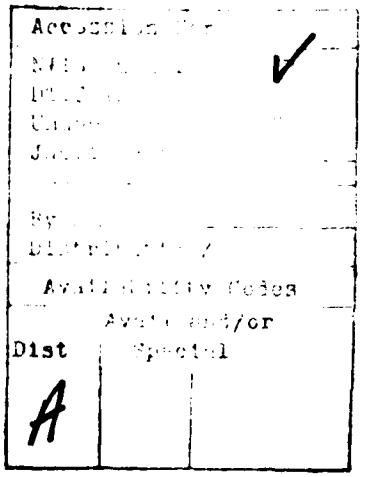

ABSTRACT

In this report, we demonstrate the use of adaptive homomorphic filtering in exposing objects under light cloud cover. More specifically, the homomorphic filter invoked is space-varying and is parameterized by the local mean level of the degraded image which serves as an indication of the extent of local cloud cover degradation. This approach represents a departure from other attempts to enhance similarly degraded images in that they have relied on nonadaptive (long-space) homomorphic filtering.

We show through some preliminary experiments that the adaptive procedure compares favorably with long-space stochastic homomorphic filtering. In particular, adaptive homomorphic filtering appears to have greater potential than the long-space methods in exposing objects beneath light cloud cover, while it does equally well as an adaptive high-pass filtering technique. In addition, adaptive homomorphic filtering compares favorably with an iterative homomorphic enhancement procedure which we have devised to improve results from the one-pass nonadaptive homomorphic filter.

CONTENTS

1. INTRODUCTION

In a number of different applied problems in optical imaging, a multiplicative degradation is often introduced in the imaging process. For example, an image obscured by shadows or light cloud cover can be modeled as the product of a function representing the original object or scene reflectivity and a "noise" component representing the degradation.

In such problems, the nonlinear procedure of homomorphic filtering has been used successfully in image restoration and enhancement. In particular, Oppenheim et al [1] and Fries and Modestino [2] have applied homomorphic filtering to enhance images whose fine structure has been obscured by the effects of shadows. The former procedure relies on a deterministic model of shadow formation, while the latter relies on a stochastic model which invokes a random field representation of shadows. In both approaches, a single homomorphic filter is applied to the image to be enhanced; i.e., one filter is applied on a long-space basis.

A similar long-space (stochastic) approach was taken also by Mitchell et al [3] in restoring images degraded by light cloud cover. Here a particular cloud pattern is viewed as a sample function of a random field. Based on estimated cloud statistics, a fixed, long-space homomorphic filter was applied over the entire image to expose objects under

light cloud cover. In neither of these problems (i.e., restoring images degraded by shadows or light cloud cover) were the local properties of the degraded image considered.

In this report, we take an alternate approach to the particular problem of enhancing images degraded by light cloud cover. As did Mitchell et al [3], we apply a homomorphic filter. This filter, however, is adaptive and requires local deterministic quantities; i.e., the filter is space-varying and is parameterized by the local mean level of the degraded image which serves as an indication of the extent of local cloud cover degradation. This approach is similar in style to the adaptive image enhancement and restoration techniques of Peli and Lim [4], Lim [5], Schreiber [6], and Gilkes [7].

The stochastic model of cloudy images invoked by Mitchell et al [3] is effectively the product of a function of the ideal image and a cloud transmission function defined over the entire extent of the image. Our cloudy image model, on the other hand, is deterministic in nature and relies on dividing the image into a number of overlapping windowed segments to each of which we associate a particular short-space cloud transmission function. The logarithm of each windowed segment can be divided into two approximately disjoint spectral bands: the cloud

transmission function being low-pass and a function of the image being high-pass. Although the image contains low-pass information, we shall assume it is not very significant in exposing object shapes under light cloud cover. In addition, we depart from a typical assmption that the desired image itself can be modeled as the product of illumination, a low frequency component, and reflectivity, a high frequency component. Rather, we view the illumination component in the same way as we view the reflectance component, i.e., as having an important high frequency component due to the interaction of light and ground objects [6]. Furthermore, we assume this high frequency component is approximately disjoint from the cloud transfer function which is low-pass.

To stage a fair comparison between our approach and that of Mitchell et al [7], we have attempted to exhibit the best of both techniques. Toward this end, we were led to an improvement of the latter algorithm. Specifically, this improvement invokes various iterative techniques for obtaining a better signal estimate by repeatedly updating the Wiener filter required in their algorithm. We have also included in our comparison the result of adaptive high-pass filtering and long-space deterministic homomorphic filtering.

Before proceeding with the development of our new methods and comparisons, we review some important ideas and formulate a framework for our investigations.

2. MODELING THE IMAGING PROCESS

A number of approaches to modeling the imaging process have been presented in the literature. A more difficult problem is to model the imaging process in the presence of light cloud cover. In this section, we first review one traditional approach to modeling undegraded images. Two different viewpoints are presented which rely on an illumination-reflectivity model. We then enter a stochastic framework in which a model of images degraded by light cloud cover will be discussed. Finally, we present our own deterministic interpretation of cloudy images. As we shall see in the following sections, each model of a light cloud covered image leads to a specific image enhancement procedure.

2.1 Deterministic Modeling of Undegraded Images

In the formation of images, the illumination and reflectivity are combined by a multiplication law [1]:

$$I(n,m) = i(n,m)\, r(n,m) \tag{1}$$

where i(n,m) and r(n,m) are the illuminance and reflectance components respectively. One assumption is that the illumination varies slowly (i.e., it contains mainly low frequency components) and the reflectance is sometimes dynamic and sometimes static and therefore may be regarded as containing mainly high frequency components. The logarithm operation separates the multiplicative signal into two additive components:

$$\log[I(n,m)] = \log[i(n,m)] + \log[r(n,m)] \tag{2}$$

If a linear amplifier or attenuator with gain α follows the log, the image output obtained by exponentiating $\alpha\log[I(n,m)]$is given by

$$I'(n,m) = [I(n,m)]^{\alpha} \tag{3}$$

When $\alpha < 1$, we obtain a washed out image and when $\alpha > 1$, the image is sharpened, but might be saturated [1]. Therefore, if we want to reduce

the dynamic range, which is contributed mostly by the illumination, while simultaneously increase the sharpness, which is contributed mostly by the reflectance, we should choose α as a function of frequency, i.e., $\alpha < 1$ for low frequencies and $\alpha > 1$ for high frequencies. More specifically, we would apply a two-dimensional (2-D) high-pass filter H(u,v) to the 2-D Fourier transform of log[I(n,m)]. The cross section of the shape of the required filter is illustrated in Figure 1. Exponentiating the modified Fourier transform yields an enhanced image. This procedure for image enhancement, termed homomorphic filtering, was first proposed by Oppenheim et al [1]. Since the illumination is not truly low-frequency and the reflectance consists not only of high frequency components but also of low frequency components, the output will have certain artifacts. It seems that the degree to which those artifacts are visible is strongly dependent on the way α changes from $\alpha < 1$ to $\alpha > 1$ [1].

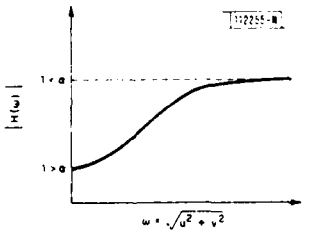

Fig. 1. Cross section of a filter with variable α.

In an alternate viewpoint, Schrieber [6] hypothesizes that in natural scenes the illumination function is as essential to perception as the reflectivity of the object. Both have a broad spectrum, generally with more power at the low spatial frequencies. The reflectance derives its low frequency component from the presence of large patches of relatively constant value. The illumination derives its high frequency component from interaction between the incident light and the edges and surfaces of objects, which are at many different angles. Consequently, any attempts to separate these components by long-space homomorphic filtering will be limited in their success. Rather, an adaptive control of the low and high frequency components at each point (along with neighboring points) of the original scene may be preferable for enhancement. Such processing, sometimes referred to as short-space processing is implemented in the system of Figure 2, as proposed by Schrieber [6]. In this general processor, we can enhance the high frequencies and reduce the dynamic range on a short-space basis in regions where it is needed. An adaptive process in this same spirit could of course be applied to the logarithm of the image, resulting in an adaptive homomorphic procedure. (It is interesting to note that Schrieber has shown that under a low-

contrast condition, a single (long-space) homomorphic filter approximates a single linear filter followed by a nonlinearity.) The sectioned method that we propose in Section 3 of this report represents a cross between the long-space homomorphic (with a single filter) and Schrieber's short-space adaptive approach (which effectively invokes a filter that is changing at each pixel).

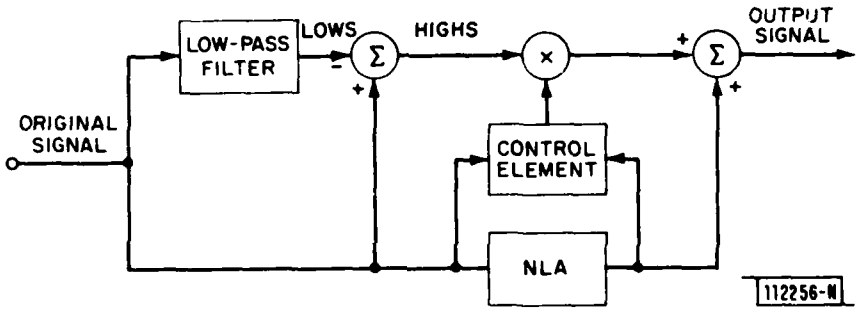

Fig. 2. Adaptive control for image enhancement.

2.2 A Stochastic Approach to Modeling Images Degraded by Light Cloud Cover

In the model of Mitchell et al [3], it is assumed that some energy of the ground reflection passes through the clouds. The energy collected above the clouds consists of two components: ground information and

scattering from the clouds. Figure 3 is a simplified model of this imaging process. The energy recorded is given by:

$$s(n,m) = aLr(n,m)t(n,m) + L[1-t(n,m)] \qquad (4)$$

where

L = sum illumination

t(n,m) = transmittance function of the cloud ($0 \leq t(n,m) \leq 1$) in a downward direction

a = attenuation of the illumination in a downward direction from the clouds to the ground (assumed constant)

r(n,m) = reflectance of the ground

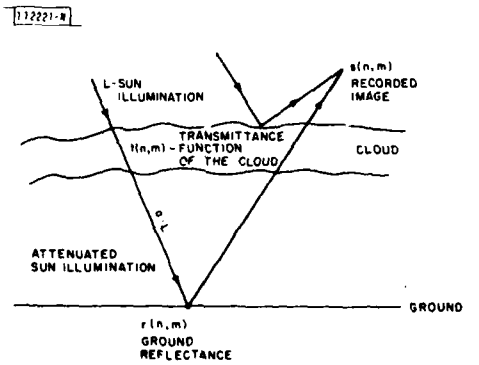

Fig. 3. A simplified model of the imaging process above clouds.

In order to recover the desired reflectance information, it was assumed that the transmittance function of the cloud and the reflectance of the ground are stochastic processes. It was also assumed that the transfer function of the cloud has relatively more energy in low spatial frequencies. From (4), we can obtain a multiplicative form of the "noise" and the "signal" given by (5):

$$L\text{-}s(n,m) = t(n,m)\,[L\text{-}aLr(n,m)] \tag{5}$$

By taking the log of (5), we obtain the addition of the "signal" and "noise" which can be written as

$$\log[L\text{-}s(n,m)] = \log[t(n,m)] + \log[L\text{-}aLr(n,m)] \tag{6a}$$

or

$$P(n,m) = N(n,m) + M(n,m) \tag{6b}$$

where

$P(n,m) = \log\,[L\text{-}s(n,m)]$ = "signal + noise"

$N(n,m) = \log[t(n,m)]$ = "noise"

$M(n,m) = \log[L\text{-}aLr(n,m)]$ = "signal"

and where $P(n,m)$, $N(n,m)$ and $M(n,m)$ are viewed as stochastic processes.

One approach to estimating the signal from (6) involves the application of Wiener filtering. If we assume that the signal and the noise are uncorrelated (a reasonable assumption here since the formation of clouds has effectively no correlation with the formation of the ground images), we can obtain the minimum mean square error estimate of the signal by filtering the given degraded image with the following optimal linear filter:

$$H(u,v) = S_{MP}(u,v) \;/\; S_{PP}(u,v)$$

$$= [S_{PP}(u,v) - S_{NN}(u,v) - M_N M_M\, \delta(u,v)] \;/\; S_{PP}(u,v) \qquad (7)$$

where,

$S_{PP}(u,v)$ = the power spectrum of the signal plus noise

$S_{NN}(u,v)$ = the power spectrum of the noise

$S_{MP}(u,v)$ = the cross power spectrum between the signal and noise

M_M = the mean value of the signal

M_N = the mean value of the noise

$\delta(u,v)$ = the 2-D dirac delta function

Mitchell et al [3] chose to estimate $S_{PP}(u,v)$ as the magnitude squared of the 2-D discrete Fourier transform of log[L-S(n,m)] where L is estimated as the highest value in the image. $S_{NN}(u,v)$ was estimated through an estimate of t(n,m) given by

$$t(n,m) = \frac{L-s(n,m)}{L-G} \tag{8}$$

where G is a constant which ideally should equal the typical ground reflection (i.e., the average of aLr(n,m)). The power spectrum of the noise was then roughly estimated by the magnitude squared of the Fourier transform of t(n,m). Since the transfer function of the cloud transmittance was considered to possess only low frequencies, the estimate of this power spectrum was low-pass filtered. Finally, an estimate of M_N and M_M can be formed from the initial values of the correlation functions associated with the estimates of $S_{PP}(u,v)$ and $S_{NN}(u,v)$ and the relation given by (6). The cross section of the general shape of the resulting optimal filter is given in Figure 4.

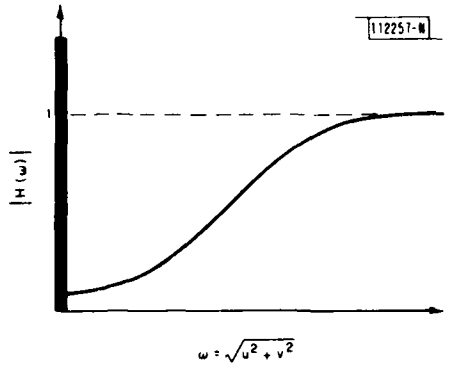

Fig. 4. Cross section of the general shape of the optimal Wiener filter.

The filter has a boost at (u,v)=(0,0) as a result of assuming a non-zero mean process and an attenuation at the low frequencies. Excluding the value at (0,0), it has the same shape as that used in the homomorphic filtering procedure of Oppenheim et al [1], described in Section 2.1 i.e., the resulting filter for the stochatic approach leads to a special case of the filter for the deterministic homomorphic approach. It should be noticed that in the stochastic approach the resulting filter is fixed for a specific image and cloud cover, while in homomorphic filtering the values of the filter at the high frequencies are variable i.e., we can increase them more than in the stochastic approach.

2.3 A Deterministic Approach to Modeling Cloudy Images

Our approach to the problem of modeling cloudy images invokes the assumption that images and clouds are deterministic processes. First we adopt Schreiber's approach [6] which assumes that both illumination and reflectance contain low and high components and that the high frequencies are important for perception. At the same time, we assume that the transfer function of the cloud transmittance contains only low frequencies on a short-space basis. We now interpret (6) so that t(n,m) (defined on a short-space basis) is deterministic and contains mainly low frequencies and L-aLr(n,m) is also deterministic and contains perceptually important high frequency information. By using these assumptions, the image aLr(n,m) can be estimated in a deterministic fashion through homomorphic filtering which reduces the low-frequency contribution of t(n,m). Furthermore, the estimate can be enhanced through homomorphic filtering by amplifying high frequency components. We elaborate on this procedure in the next section.

3. EXTENSIONS OF HOMOMORPHIC FILTERING

The assumption that clouds are stationary and approximately low-pass motivated the long-space stochastic homomorphic filtering approach of Mitchell et al [3]. However, the thickness of cloud cover certainly does change over the extent of an image, and, as we stated in the previous section, seems to exhibit rather deterministic properties. Consequently, an adaptive approach should be better suited to restoring the desired image, i.e., an approach where the homomorphic filter changes with local cloud characteristics which are viewed as non-stationary in nature.

Before proceeding with this adaptive processing, in order to make a fair comparison, we shall first do the best we possibly can with the stochastic long-space approach of Mitchell et al. The improvement that we achieve in their procedure relies on an iterative method of estimating cloud statistics (this method in fact has been suggested but was never implemented [3]).

3.1 The Stochastic Iterative Approach

We saw in Section 2.2 that a cloudy image can be modeled (after a log transformation) as a sum of noise and signal reflectivity components given in (6). Note that this model assumes that illumination reaching the ground hits objects uniformly. We saw, however, that it is not precisely true due to the different angular arrangement of objects. Nevertheless, this effect will be assumed lumped into the function r(n,m), since as noted in Section 2, the resulting illumination will contain an important high frequency component.

The objective of Section 2.2 was to obtain an optimal estimate of the term log[L-aLr(n,m)] in the presence of the "colored noise" term log[t(n,m)]. We found that we could do this theoretically by applying a Wiener filter of the form

$$H(u,v) = S_{MP}(u,v) \;/\; S_{PP}(u,v) \qquad (9)$$
$$= [S_{PP}(u,v) - S_{NN}(u,v) - M_N M_M \,\delta(u,v)] \;/\; S_{PP}(u,v)$$

where the components of (9) are defined in Section 2.2. $S_{PP}(u,v)$ was approximated by the squared magnitude of the Fourier transform of the noisy signal, and $S_{NN}(u,v)$ was given by the crude approximation given in (8).

An alternative approach involves iteratively updating the estimate of the spectral density of the clouds. Since an estimate of the reflectance function aLr(n,m) is required for the cloud spectral density (see(8)), we can use an estimate of aLr(n,m) to update the estimate of the cloud spectral density. The Wiener filter in (9) is then updated and the original cloudy image is again filtered. If we do this repeatedly, the resulting iterative process may converge to a better estimate than generated by the one step process. In the space domain, the initial cloud estimate is given by

$$t_1(n,m) = \frac{L-s(n,m)}{L-G_0} \qquad (10.a)$$

where G_0 is a constant (see Section 2.2). From $t_1(n,m)$, we obtain a better estimate of aLr(n,m) denoted by $G_1(n,m)$, and the iteration is continued as

$$t_{k+1}(n,m) = \frac{L-s(n,m)}{L-G_k(n,m)} \qquad (10.b)$$

where $G_k(n,m)$ is the kth estimate of the function aLr(n,m). Figure 5 outlines the procedure. Figure 6 illustrates a modification of this it-

eration where rather than filtering the original cloudy image on each iteration we filter the updated signal estimate (i.e., filter $G_{k+1}(n,m)$ by using $G_k(n,m)$ to create the new signal estimate $G_{k+2}(n,m)$). In the space domain, the iterative cloud estimate is given by

$$t_{k+2}(n,m) = \frac{L-G_{k+1}(n,m)}{L-G_k(n,m)} \qquad k=1,... \tag{11.a}$$

The initial conditions $t_1(n,m)$ and $t_2(n,m)$ are generated as

$$t_1(n,m) = \frac{L-s(n,m)}{L-G_0} \tag{11.b}$$

where G_0 is a constant

and

$$t_2(n,m) = \frac{L-s(n,m)}{L-G_1(n,m)} \tag{11.c}$$

In theory, this procedure is not as sound as that which filters the original noisy signal, but as we will see, it appears to generate a better restoration. Since $G_{k+1}(n,m)$ is a better estimate than $G_k(n,m)$ of the original image, we might use it to obtain a better estimate of the cloud transmittance in order to filter $G_k(n,m)$ (i.e., swap $G_{k+1}(n,m)$ and $G_k(n,m)$ in 11.a).

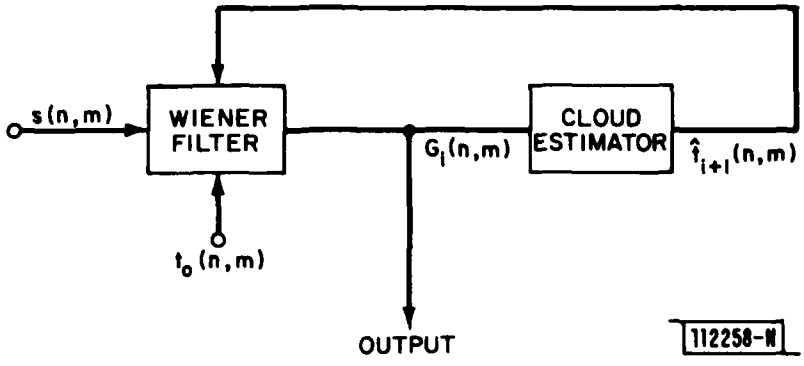

Fig. 5. Iterative procedure which operates on the original cloudy image.

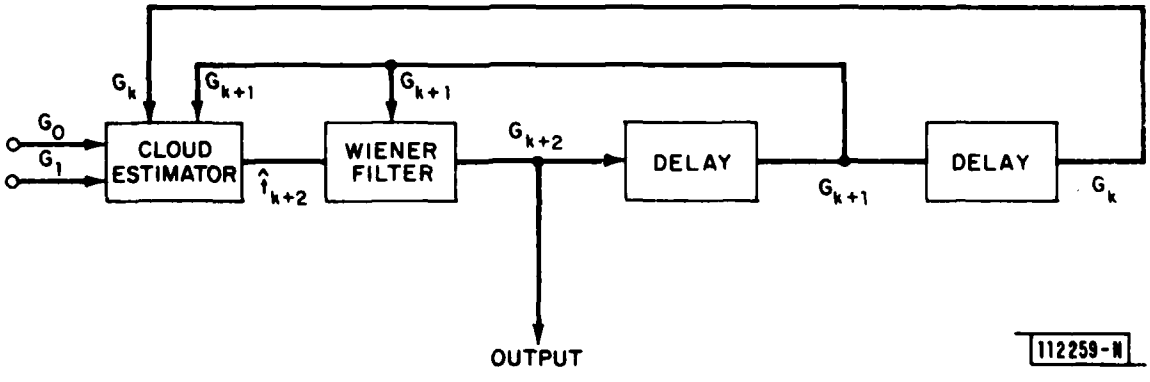

Fig. 6. Iterative procedure which operates on an updated image estimate.

3.2 The Deterministic Adaptive Approach

Consider now applying a short-space window to the noisy signal P(n,m) in (6). More specifically, let's assume the window takes on a pyramidal shape, has a MxM square region of support, and is shifted over the data at intervals of half its width (i.e., M/2) in both the n and m directions. If w(n,m) denotes the pyramidal window centered at the origin, then a particular windowed segment takes on the form:

$$P_{j,k}(n,m) = w(n-jM/2,\ m-kM/2)P(n,m) \tag{12}$$

where the window w(n,m) has the following desirable property:

$$\sum_j \sum_k w(n-jM/2,\ m-kM/2) = 1 \tag{13}$$

Consequently, the sectioning procedure is reversible; i.e., if no processing is applied to each section, then the image can be recovered exactly.

Applying an adaptive filter which operates on each segment $P_{j,k}(n,m)$, we obtain

$$\hat{P}_{j,k}(n,m) = P_{j,k}(n,m) ** h_{j,k}(n,m,\alpha) \tag{14}$$

$$= [w(n-jM/2,m-kM/2)P(n,m)] ** h_{j,k}(n,m,\alpha)$$

where the parameterized filter impulse response $h_{j,k}(n,m,\alpha)$ is a function of the vector α, which is a set of parameters dependent on the local cloud characteristics. In particular, α is a function of the DC level of the windowed signal which reflects the cloud density under the window. Further, the filter is high-pass where the shape and amplitude-depend on α. The following section will elaborate on this design. From (6), the filtering process is then given by

$$\hat{P}_{j,k}(n,m) = [w(n-jM/2,\ m-kM/2)[\log(t(n,m)+\log(L-aLr(n,m))]] \\ **h_{j,k}(n,m,\alpha) \qquad (15)$$

We assume that the window is "sufficiently smooth" so that the low-pass nature of the noise term log[t(n,m)] and the high-pass nature of the signal component log[L-aLr(n,m)] are preserved after windowing. Consider now the case where the noise and the signal are exactly disjoint in frequency, and the filter $h_{j,k}(n,m,\alpha)$ is an ideal high-pass filter whose non-zero energy band matches that of the signal. Then we can write

$$\hat{P}_{j,k}(n,m) = w(n-jM/2,\ m-kM/2)\ \log[L-aLr(n,m)] \qquad (16)$$

Since the noise and signal are only approximately disjoint, the noise term will not be entirely removed, and since the filter is not an ideal high-pass, the signal will not remain intact. Alternately, when $h_{j,k}(n,m,\alpha)$ adaptively amplifies the high frequencies and attenuates the low frequencies, the cloud will only be partially suppressed (while also changing the low frequency component of log(L-aLr(n,m))*) and the high frequency detail of the desired signal will be enhanced** (while boosting any cloud energy in this region). The relation in (16) is then only an approximation which represents an estimate of the desired windowed signal (or desired enhanced signal) along with the effects of any residual cloud noise. The parameters α, in $h_{j,k}(n,m,\alpha)$, which rely on the local cloud density should be chosen so that the noise is suppressed as much as possible, while the estimate of the undegraded image is optimal in some sense.

---

* We assume, however, that these components are not perceptually important.

** As shown in the following section, under a low contrast condition (i.e., with thick clouds) and with a filter magnitude greater than unity in high-frequency regions, the local constrast will be enhanced.

With these approximations in mind, our reconstruction procedure which we refer to as overlap-add can then, with the use of (13), be written as

$$P(n,m) = \sum_j \sum_k w(n-Mj/2,\ m-Mk/2)\ \log(L-aLr(n,m))$$

$$= \log[L-aLr(n,m)] \sum_j \sum_k w(n-Mj/2,\ m-Mk/2) \qquad (17)$$

$$= \log[L-aLr(n,m)]$$

This procedure is illustrated in Figure 7. Finally, to obtain an estimate of the signal, we exponentiate and recover aLr(n,m) from log[L-aLr(n,m)].

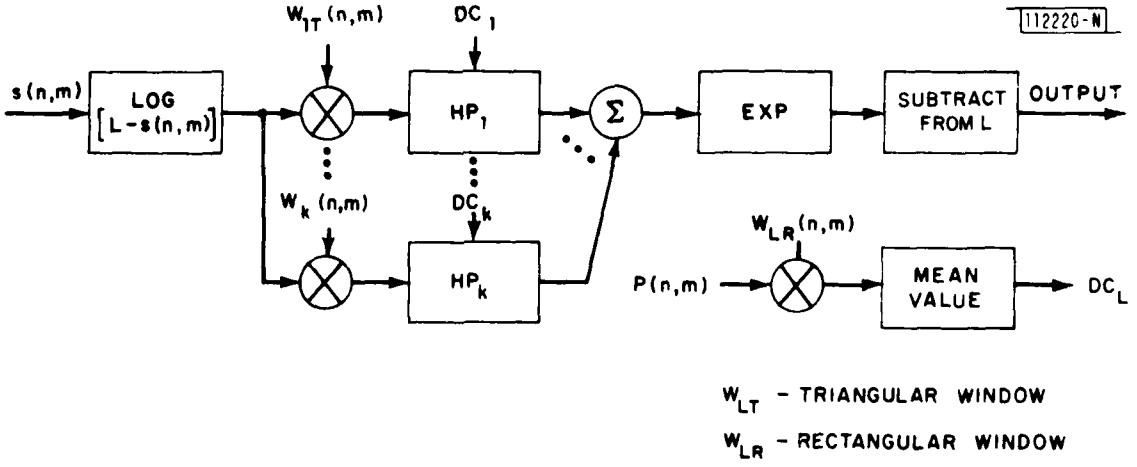

Fig. 7. Image restoration by deterministic homomorphic filtering.

3.3 Filter Design

From the simple model of imaging above clouds, we have concluded that it is desirable to adaptively attenuate the low frequencies and to amplify the high-frequencies of log [L-s(n,m)] given in (6). In order to proceed with the high-pass filter design, let's first look more carefully at the process of filtering (6) adaptively. To simplify the complications due to the logarithmic operation, we shall approximate (6) by its Taylor series expansion. This is an accurate approximation under a low contrast condition. In addition, we shall extend the model in (6) by allowing the downward attenuation factor a to take on a space-varying characteristic of the form a(n,m). This generalization accounts for the possible changes in illumination reaching the ground due to the varying atmospheric and other effects from the clouds to the ground. Thus, we account for a varying cloud thickness through t(n,m) and other nonstationary effects (i.e., fog, haze, etc.) through a(n,m).

The windowed segment in (15) then becomes :

$$\hat{P}_{j,k}(n,m) \cong w_{j,k}(n,m)\,[\log[t(n,m)] + \log[L] + a(n,m)r(n,m)] \qquad (18)$$

If $t(n,m)$ and $a(n,m)$ are slowly-varying over the window $w_{j,k}(n,m)$, then in the frequency domain our filter should decrease the large negative low frequencies of the Fourier transform of $\log[t(n,m)]$ and should increase the highs because of the attenuation of $r(n,m)$ which holds perceptually important high-frequency information. Returning to (4), we see that we have effectively enhanced the local contrast in areas of thick clouds by reducing the shift in the local brightness level from light bouncing off clouds, and by compensating for local attenuation from passage of light through clouds.

Our filter, therefore, should be high-pass with three specific desirable characteristics. First, the high-frequency end of the filter should increase monotonically as the cloud thickness increases. Furthermore, we may wish to overcompensate for high-frequency loss (i.e., enhance rather than simply restore the image) by boosting the highs beyond what would occur in an undegraded (cloudless) image. Secondly, we want also to increase the low-frequency end with increasing cloud thickness. This will, in effect, decrease the low-frequency negative contribution due to the $\log[t(n,m)]$ component. We note that it may be desirable to alter the high-pass filter so that there exists a narrow pulse at DC to

accomplish the low-frequency boost*. We found, however, that this filter characteristic was not necessary to achieve high-quality results. Finally, we may also wish to broaden the bandwidth of the filter in the high-frequency range as the cloud thickens to compensate for other forms of high-frequency loss, as for example blurring due to the scattering of light through clouds. A filter which has the desirable shape and is computationally efficient is a circularly symmetric Gaussian which is shifted to $(u,v)=(\pi,\pi)$. A cross section of this filter is shown in Figure 8 and the filter is given by

$$H(u,v) = A \exp\left[-\left(\frac{u-\pi}{B}\right)^2 - \left(\frac{v-\pi}{B}\right)^2\right] + C \qquad (19)$$

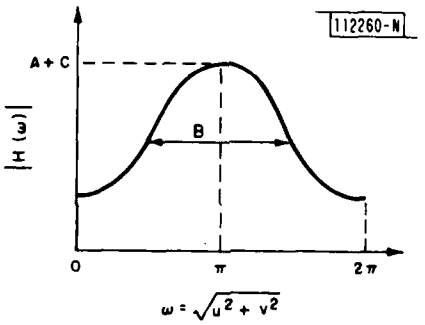

Fig. 8. Cross section of the desired high-pass filter.

* The resulting bimodal filter then resembles that derived through the stochastic approach of Mitchell et al [3].

The filter size was chosen to be fixed at 16x16. The filter parameters A, B, and C are functions of the value of the Fourier transform of the windowed data at DC, i.e., at $(u,v)=(0,0)$, which is an indication of the cloud thickness. To determine the parameters, we first specify the values at $(u,v)=(0,0)$ and at $(u,v)=(\pi,\pi)$ for DC=0 and for DC=255. Each of the two pairs (i.e., one pair for the value at $(u,v)=(0,0)$ for DC=0 and DC=255 and the other pair than for the value at $(u,v)=(\pi,\pi)$ for DC=0 and DC=255), is then quadratically interpolated according to the formula

$$Y = (Y_2 - Y_1)\, D^2 / 255^2 + Y_1 \qquad (20)$$

where D denotes the DC level which takes on values from 0 to 255 and where Y_2 and Y_1 denote two extreme values, one at $(u,v)=(0,0)$ and the other at $(u,v)=(\pi,\pi)$. This yields the filter endpoints for DC levels between 0 and 255. A quadratic interpolation for computing the desired intermediate values was used rather than a linear interpolation because a larger range of low level of luminance needs almost no processing. The filter parameters A and C in (19) are then chosen so that the filter meets these computed endpoints. The parameter B in (19) is computed directly in terms of the quadratic interpolation formula (20) and two desired extreme values.

4. EXPERIMENTAL RESULTS

4.1 Stochastic Approach (original + iterative)

This experiment was performed in order to compare the stochastic approach to the various deterministic procedures. Figure 9 is the result of the algorithm of Mitchell et al where the estimate of the typical ground reflection G(n,m) was chosen to be a constant equal to 140. The processed image seems to contain primarily the high frequencies of the unprocessed image.

By using the iterative approach of (10), one can improve the estimate of the noise spectrum. Figure 10.a contains the result after 3 iterations. Figure 10.b illustrates the result after three iterations which improve the estimate of the noise while processing the image estimate itself (see the iterative procedure given in (11)). One can see that the second form of iteration appears to yield a perceptually more desirable result. Finally, Figure 10.c depicts the result after using 4 it-

erations of (11), but where $G_{k+1}(n,m)$ is used to process $G_k(n,m)$ (i.e., $G_{K+1}(n,m)$ and $G_k(n,m)$ in (11) are swapped). All the results (Fig. 9 - Fig. 10) are presented after histogram equalization.

(a) (b)

Fig. 9. a) An original cloudy image b) The result of the stochastic approach

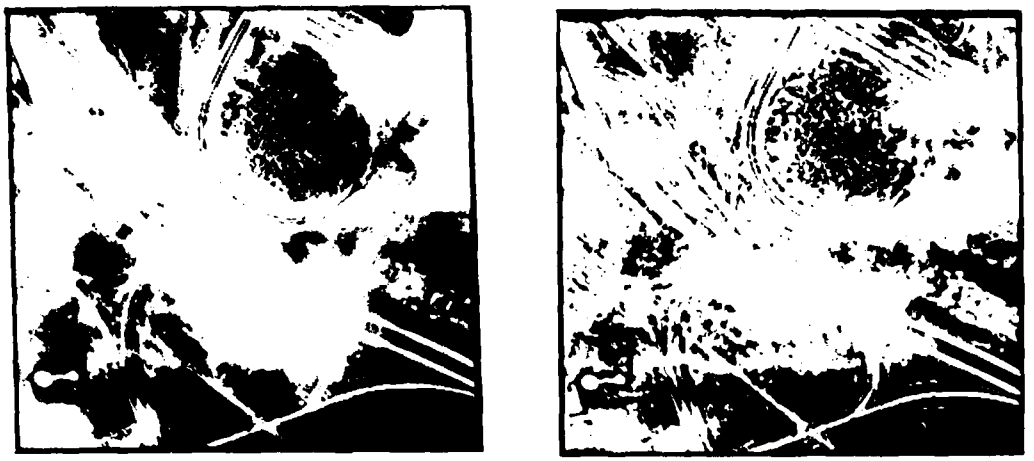

(a) (b)

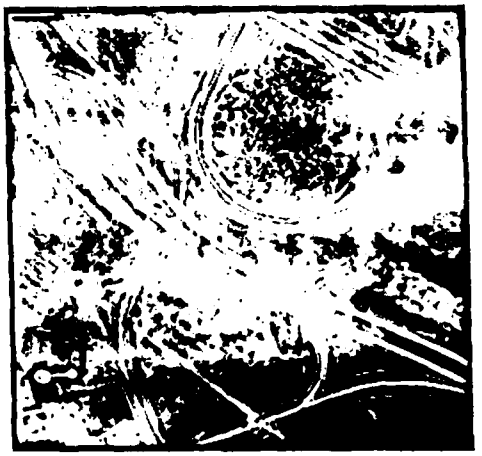

(c)

Fig. 10. a) Result of using the iteration in (10). b) Result of using the iteration in (11). c) Result of using (11) but where $G_{k+1}(n,m)$ is used to process $G_k(n,m)$.

4.2 Long Space Homomorphic Filtering (Deterministic)

In this section, long-space homomorphic filtering was examined with two different filters. Each has a Gaussian shape as described in Section 3.2. The parameters of the first filter are A=3.65, B=320, and C=-2.15 and its shape is given in Figure 11. The result is illustrated in Figure 12.

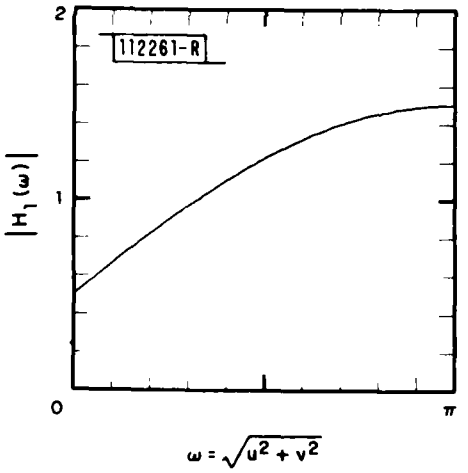

Fig. 11. Cross section of the filter used in the long space homomorphic filtering

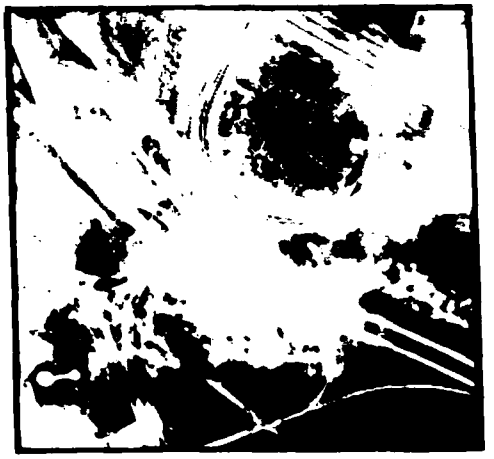

Fig. 12. Result of the long space homomorphic filtering by using $H_1(\omega)$ in Fig. 11.

The second filter, which sharpens and attenuates more than the first, has the shape and parameters given in Figure 13 and the processed image is illustrated in Figure 14. The two results are presented after histogram equalization. From these results, we can see that there is some sharpening but most of the cloud was not removed and, therefore, some objects were not exposed.

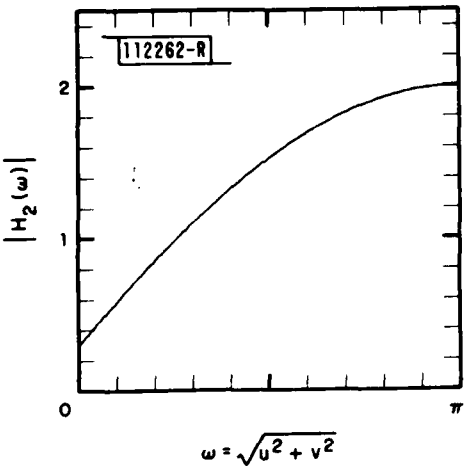

Fig. 13. Cross section of the filter used in the long space homomorphic filtering.

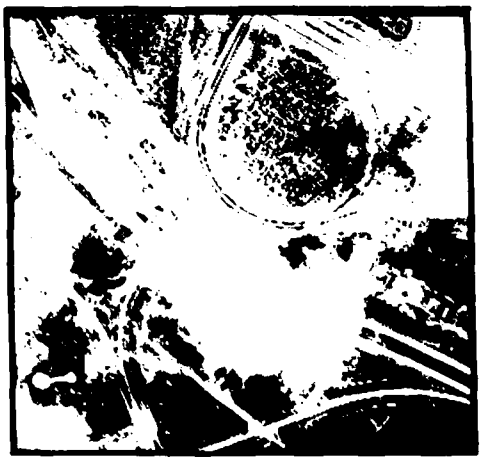

Fig. 14. Result of the long space homomorphic filtering by using $H_2(\omega)$ in Fig. 13.

The value at (u,v)=(0,0) for the two filters is less than one although theoretically it should be greater than one as in the adaptive homomorphic approach. Since we apply the filter on a long space basis and rescale the result into the range of 0-255, only the relation of H(0,0) to H(π, π) is important as illustrated in Figure 15.

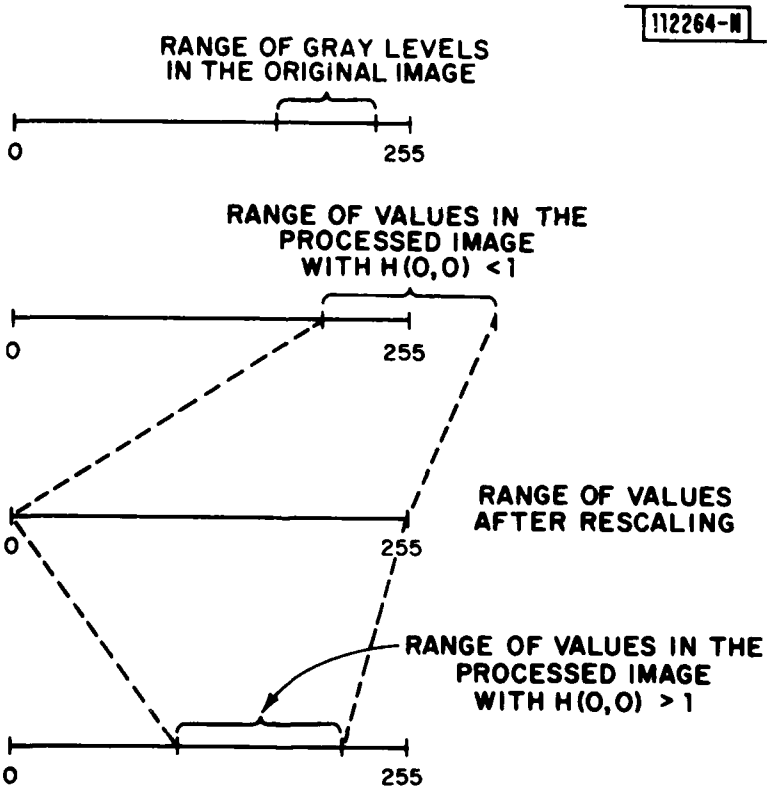

Fig. 15. An example that illustrates the importance of the relation between H(0,0) and H(π,π).

4.3 Adaptive Homomorphic Filtering

In this approach, a pyramidal window of size 16x16 was chosen and the range of parameters is given in Table I. Table I requires some elaboration. First, we choose to allow the value of the filter at (u,v)=(0,0) to take on values less than unity in order to brighten extremely dark areas of the specific image which we are processing. Recall from Section 3.3 that the signal is log[L-S(n,m)] (i.e., bright regions are transformed into dark regions and vice versa). In such a case an increase in the value of the high-pass filter at (0,0) lowers the resulting mean level of the image in the space domain). Secondly, in order not to over-brighten the very dark areas of the image we have set the value of the filter at (u,v)=(0,0) to about 0.8 for all values of DC less than 170, thus not allowing the lower limit of 0.53 to be reached. These parameter values were obtained after some exhaustive twiddling to obtain an "optimal" enhancement. We should note that the quality of the resulting enhanced image appears to exhibit a large sensitivity to small perturbations in the chosen parameters.

The local filter was generated by interpolating between the two extreme filters (shown in Fig. 16) according to the interpolation formula given in (20). The result after histogram equalization is illustrated in Figure 17.

TABLE 1

RANGE OF PARAMETERS FOR THE ADAPTIVE HOMOMORPHIC FILTER

DC	0	255
(π,π)	1.1	1.5
$(0,0)$	0.53	1.2
B	5	20

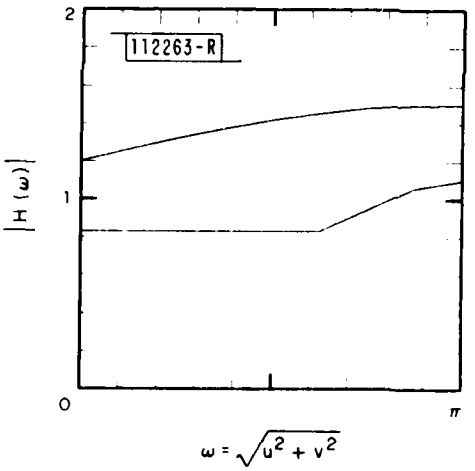

Fig. 16. Two extreme filter shapes which define the limits of the local filters used in the adaptive homomorphic filtering approach.

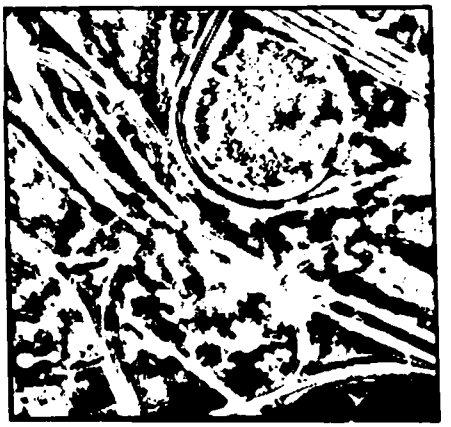

Fig. 17. The cloudy image processed by the adaptive homomorphic filter given in Fig. 16.

4.4 Adaptive High-Pass Filtering

In the final experiment, we applied adaptive high-pass filtering to the windowed image s(n,m) in (4), rather than the windowed logarithm of (L-s(n,m)) in (6). The high frequency end (i.e., (u,v)=(,)) of the high-pass filter was increased monotomically with cloud thickness, while the low-end (i.e., (u,v)=(0, 0)) was decreased monotonically. It should be pointed out that these parameter choices were based on the additive model of (4) rather than the multiplicative model of (5)*. The extreme filter values (again chosen by twiddling) and the resulting enhanced image after histogram equalization are depicted in Table II and Figure 18, respectively. From Figure 18 one can see the result is sharper than the result from adaptive homomorphic filtering but exhibits more noise especially in the darker regions.

---

* Nevertheless, applying a nonlinearity (for dynamic range manipulation) in cascade with a high-pass filter, from Schrieber's studies [6], we suspect that under a low-contrast condition, the resulting enhanced image should approach that obtained from adaptive homomorphic filtering.

Fig. 18. The cloudy image processed by the adaptive high-pass filter given in Table II.

TABLE II

RANGE OF PARAMETERS FOR THE ADAPTIVE HIGH PASS FILTER

DC	0	255
(π,π)	0.3	1.8
(0,0)	0.9	1.1
B	5	20

4.5 Conclusions

In this section, we have presented some informal preliminary experimental results to illustrate the various enhancement procedures which were proposed in the earlier sections of this report. Inspection of Figures 9 through 17 illustrates that the adaptive homomorphic procedure does better in removing light cloud cover (i.e., in exposing objects under light cloud cover) than does the stochastic iterative or long-space homomorphic approach.

Furthermore, the adaptive homomorphic procedure appears to yield a less noisy result since a very high-frequency gain is not applied over the entire image. On the other hand, the result from the adaptive homomorphic procedure contains less high-frequency detail and somewhat more low-frequency "patchiness" (probably due to the sensitivity of the local mean level arising from the nonlinear logarithmic operation) than that from the two non-adaptive techniuques.

When compared with the adaptive high-pass, the adaptive homomorphic yields a less noisy result, but also with less high-frequency detail, particularly in darker regions. This is probably due to the fact that

in adaptive high-pass filtering, the high-frequency gain is applied directly to the image, and thus its effect is not (potentially) attenuated by the presence of a nonlinearity. Finally, the adaptive homomorphic procedure appears to do as well as the adaptive high-pass algorithm in exposing objects under light cloud cover.

5. SUMMARY AND DISCUSSION

In this report, we have demonstrated the use of adaptive homomorphic filtering in exposing objects under light cloud cover. The adaptive filter is high-pass in nature and is parameterized by the local mean level of the degraded image which serves as an indication of the extent of the local cloud cover.

We have shown through some preliminary experiments that this approach compares favorably with the long-space stochastic (iterative) and homomorphic approaches. More specifically, the adaptive homomorphic procedure appears to have a greater potential than the long-space methods in exposing objects beneath light cloud cover while it does equally well as the adaptive high-pass technique. Furthermore, while the adaptive homo-

morphic scheme does well in suppressing high-frequency noise, it exhibited less high-frequency detail than the additive high-pass filtering procedure.

This report has generated a number of additional questions. Specifically, developing methods to suppress noise while exposing objects (and enhancing the detail of these objects) is of paramount importance. The adaptive homomorphic scheme appears to have a greater potential in suppressing noise than for example adaptive high-pass filtering. One possible reason for this is that adaptive homomorphic filtering performs local contrast enhancement on a nonlinear function of the image while the adaptive high-pass filtering can be approximated by a differentiation operation applied directly to the image.

Another important question involves the way in which the image is segmented. We have in this report divided the image into overlapping square segments. An alternate method is to process the image adaptively on a point-by-point basis (similar to the procedure of Peli and Lim [4]). It is important to understand the differences in these approaches, with respect to their computational and noise suppression characteristics.

REFERENCES

[1] A.V. Oppenheim, R.W. Schafer and T.G. Stockham, "Nonlinear Filtering of Multiplied and Convolved Signals," Proc. IEEE, 1264, (1968).

[2] R.W. Fires and J.W. Modestino, "Image Enhancement by Stochastic Homomorphic Filtering," IEEE Trans. Acoust., Speech, and Signal Processing, ASSP-27, 625, (1979).

[3] O.R. Mitchell, E.J. Delp and P.L. Chen, "Filtering to Remove Cloud Cover in Staellite Imagery," IEEE Trans. Geosci. Electron., GE-15 137, (1977).

[4] T. Peli and J.S. Lim, "Adaptive Filtering for Image Enhancement," ICASSP, Atlanta, GA, March 1981.

[5] J.S. Lim, "Short Space Implementation of Wiener Filtering for Image Restoration," Technical Note 1980-11, Lincoln Laboratory, M.I.T. (5 March 1980, DTIC-AD A086769/7.

[6] W.F. Schreiber, "Image Processing for Quality Improvement," Proc. of the IEEE, 1650, (1978).

[7] A. Gilkes, "Photograph Enhancement by Adaptive Digital Unsharp Masking," M.S. Thesis, Massachusetts Institute of Technology, Electrical Engineering and Computer Science Department (1974).

UNCLASSIFIED

SECURITY CLASSIFICATION OF THIS PAGE (When Data Entered)

REPORT DOCUMENTATION PAGE		READ INSTRUCTIONS BEFORE COMPLETING FORM
1. REPORT NUMBER ESD-TR-81-363	2. GOVT ACCESSION NO.	3. RECIPIENT'S CATALOG NUMBER
4. TITLE (and Subtitle) Exposing Objects Under Light Cloud Cover by Adaptive Homomorphic Filtering		5. TYPE OF REPORT & PERIOD COVERED Technical Report 6. PERFORMING ORG. REPORT NUMBER Technical Report 587
7. AUTHOR(s) Tamar Peli and Thomas F. Quatieri		8. CONTRACT OR GRANT NUMBER(s) F19628-80-C-0002
9. PERFORMING ORGANIZATION NAME AND ADDRESS Lincoln Laboratory, M.I.T. P.O. Box 73 Lexington, MA 02173		10. PROGRAM ELEMENT, PROJECT, TASK AREA & WORK UNIT NUMBERS Program Element No. 62702F Project No. 4594
11. CONTROLLING OFFICE NAME AND ADDRESS Rome Air Development Center Griffiss AFB, NY 13440		12. REPORT DATE 6 January 1982 13. NUMBER OF PAGES 48
14. MONITORING AGENCY NAME & ADDRESS (if different from Controlling Office) Electronic Systems Division Hanscom AFB, MA 01731		15. SECURITY CLASS. (of this report) Unclassified 15a. DECLASSIFICATION DOWNGRADING SCHEDULE

16. DISTRIBUTION STATEMENT (of this Report)

Approved for public release; distribution unlimited.

17. DISTRIBUTION STATEMENT (of the abstract entered in Block 20, if different from Report)

18. SUPPLEMENTARY NOTES

None

19. KEY WORDS (Continue on reverse side if necessary and identify by block number)

adaptive filtering	homomorphic filtering	short space processing
image enhancement	iterative processing	light cloud degradation

20. ABSTRACT (Continue on reverse side if necessary and identify by block number)

In this report, we demonstrate the use of adaptive homomorphic filtering in exposing objects under light cloud cover. More specifically, the homomorphic filter invoked is space-varying and is parameterized by the local mean level of the degraded image which serves as an indication of the extent of local cloud cover degradation. We show through some preliminary experiments that this approach compares favorably with long space methods such as deterministic and stochastic homomorphic filtering and an iterative version of stochastic homomorphic filtering.

DD FORM 1 JAN 73 1473 EDITION OF 1 NOV 65 IS OBSOLETE

UNCLASSIFIED

SECURITY CLASSIFICATION OF THIS PAGE (When Data Entered)

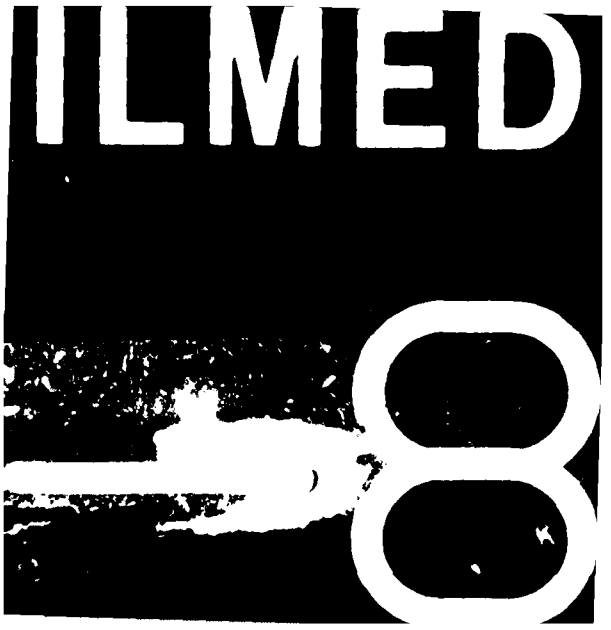
ILMED
8